3rd Specialty Conference on Material Engineering & Applied Mechanics
3e Conférence spécialisée sur le génie des matériaux et mécanique appliquée

Montréal, Québec
May 29 to June 1, 2013 / *29 mai au 1 juin 2013*

Characterization of Basalt Fiber-Reinforced Polymer (BFRP) Reinforcing Bars for Concrete Structures

Patrick Vincent, Ehab Ahmed, and Brahim Benmokrane
Department of Civil Engineering, University of Sherbrooke, Sherbrooke, Quebec, Canada

Abstract: Due to non-corrodible nature, fiber-reinforced polymers (FRP) materials are being used as main reinforcement in reinforced and prestressed concrete structures subjected to harsh environmental conditions such as bridge decks and barriers, parking garages, and marine structures. The enhancement in manufacturing techniques yielded new generations of FRP bars and provided a step forward to utilize different fiber types, such as basalt fibers, rather than the commonly used fibers. However, investigations are needed to evaluate the short- and long-term characteristics of these new FRP bars. This investigation aims at characterizing newly developed basalt fiber-reinforced polymer (BFRP) bars and evaluating the bond-dependent coefficient (k_b) of these bars. The investigation included physical and mechanical characterization of sand-coated BFRP bars of 10, 12, and 16 mm-diameters. In addition, 3 beams reinforced with sand-coated BFRP bars of 10, 12, and 16 mm-diameters were constructed and tested to evaluate the bond-dependent coefficient (k_b) and compare it with the current design recommendations of the FRP design codes and guides. The test results confirmed that the developed BFRP bars meet the requirements of the CSA S807-10 concerning their physical and mechanical properties. Furthermore, the preliminary beam testing proposed a bond-dependent coefficient (k_b) of 0.8 for the tested BFRP bars.

1 Introduction

Fiber-reinforced-polymer (FRP) bars are corrosion resistant by nature and have been used for decades in concrete structures and bridges to eliminate the steel corrosion and related deterioration problems. With advances in manufacturing techniques and technology, FRP bars are being produced with enhanced properties. In addition, ACI 440 (2008) and CSA S807 (2010) provided a step forward in standardizing the FRP bars manufactured with glass, carbon and aramid fibers. This is expected to increase the applications of FRP reinforcement in concrete infrastructure.

Given the recent research in the textile/fiber industry, the basalt fiber showed a great potential as a competitive for glass fiber. This study aims at characterizing newly developed basalt fiber-reinforced polymers (BFRP) bars and evaluating their bond-dependent coefficient (k_b). This study will help in introducing FRP bars made with basalt fibers in the available Canadian Codes and Standards such as CSA S806, CSA S6 and CSA S807.

2 Experimental Program Outline

This study includes an experimental investigation to characterize newly developed basalt FRP bars (BFRP). The bars have a sand-coated surface over helical wire wrapping as shown in Figure 1. The investigation includes complete physical and mechanical characterization of three diameters of these

BFRP bars (10, 12, and 16 mm). The characterization is conducted in accordance with the ACI 440 (2008) and CSA S807 (2010). In addition, the bond-dependent coefficient (k_b), as one of the important design parameters, is evaluated and compared with the available design recommendations for FRP bars. The evaluation of k_b is conducted according to Annex S of the CSA S806 (2012) "*Test Method for Determining the Bond-Dependent Coefficient of FRP Rods.*"

Figure 1: Basalt FRP bars

3 Physical Characterization

The physical properties of the BFRP bars were conducted in accordance with ACI 440 (2008) and CSA S807 (2010). The effective cross-sectional area was determined following CSA S806 (2012), Annex A *"Determination of Cross-Sectional Area of FRP Reinforcement".* The fiber content was determined according to ASTM D3171 (2011) *"Standard Test Method for Constituent Content of Composite - Method I; Procedure G*". The transverse coefficient of thermal expansion was determined according to ASTM E831 (2012) *"Standard Test Method for Linear Thermal Expansion of Solids Materials by Thermomechanical Analysis".* The water absorption was determined according to ASTM D570 (2010) *"Standard Test Method for Water Absorption of Plastics".* The cure ratio was determined according to ASTM D5028 (2009) *"Standard Test Method for Curing Properties of Pultrusion Resin by Thermal Analysis".* The glass transition temperature (T_g) was determined according to ASTM D3418 (2012) *"Standard Test Method for Transition Temperatures of Polymers by Thermal Analysis".* It should be mentioned that the void content ratio was not measured because of the unavailable data concerning the densities of the fibers and the resin. Table 1 presents the results of those physical characterization tests and compare them against the specified limits of ACI 440 (2008) and CSA S807 (2010). The comparison presented in Table 1 confirms that the newly developed BFRP bars tested herein meet the physical properties requirements of ACI 440 (2008) and CSA S807 (2010).

4 Mechanical Characterization

The mechanical characterization conducted herein included tensile test, transverse shear strength test, and pullout test. The tensile properties of the BFRP bars were determined by testing of five specimens in accordance with CSA S806 (2012), Annex C *"Test Method for Tensile Properties of FRP Reinforcement".* Figure 2 shows a typical tensile test and mode of failure of the tested BFRP bars. The transverse shear strength were determined in accordance with ASTM D7617 (2011) "*Standard Test Method for Transverse Shear Strength of Fiber-Reinforced Polymer Matrix Composite Bars*". Figure 3 shows the transverse

shear strength test and a photo for the typical mode of failure of the BFRP bars. The pullout tests were carried out in normal-strength concrete according to ACI 440 (2004), B.3 Test Method "*Test Method for Bond Strength of FRP Bars by Pullout Testing*" and CSA S806 (2012), Annex G "*Test Method for Bond Strength of FRP Rods by Pullout Testing*". The bonded length was kept constant at $5d_b$, where d_b is the FRP bar diameter. Figure 4 shows the geometry of the pullout specimens, test setup, and mode of failure. The complete description of the mechanical properties of the BFRP bars is presented in Table 2.

Table 1: Specified limits and results for physical properties of BFRP bars

Property	Specified limit		Measured		
	ACI 440 (2008)	CSA S807 (2010)	10 mm	12 mm	16 mm
Basalt fiber content	55% (by vol.)	70% (by w.)	87.2% (by w.) ~ 75 % (by v.)	90.6% (by w.) ~ 81% (by v.)	89.9% (by w.) ~ 79 % (by v.)
Transverse CTE	NA	$40{\cdot}10^{-6}$ °C^{-1}	$22.2{\cdot}10^{-6}$ °C^{-1}	$23.0{\cdot}10^{-6}$ °C^{-1}	$25.8{\cdot}10^{-6}$ °C^{-1}
Void content	NA	1 %	ND	ND	ND
Water absorption at saturation	1 %	1.0 % (D2) 0.75% (D1)	0.18 %	0.16 %	0.21 %
Cure ratio	NA	93% (D2) 95% (D1)	100 %	100 %	100 %
Glass transition temperature (T_g)	100°C	80°C (D2) 100°C (D1)	111°C	103°C	116°C

(a)  (b) 

Figure 2: Typical tensile test: (a) Test setup; (b) Typical tension failure

(a)  (b) 

Figure 3: Transverse shear strength test: (a) Test setup; (b) Typical shear failure

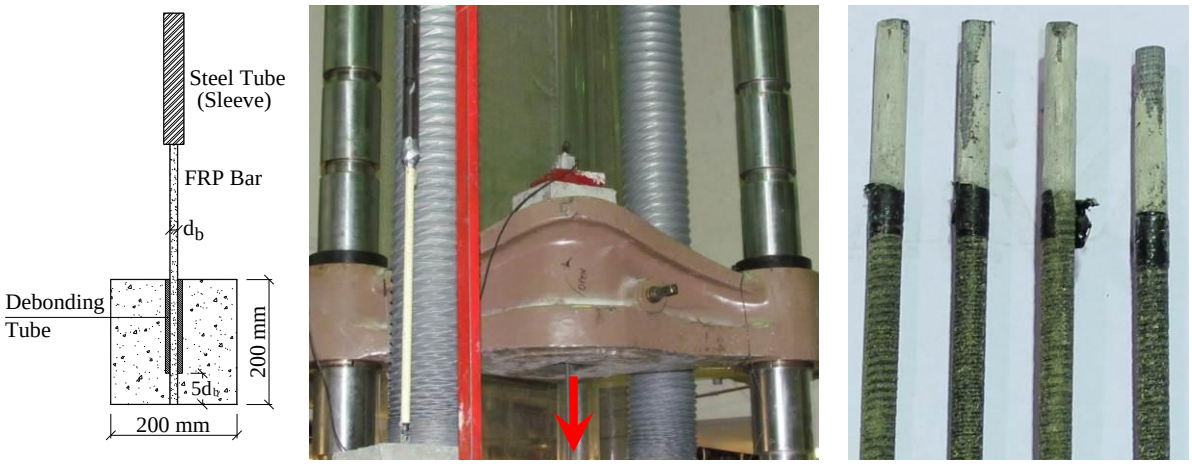

(a) (b) (c)

Figure 4: Pullout test: (a) Geometry of the specimens; (b) Test setup; (c) Mode of failure

Table 2: Mechanical properties of BFRP bars

Diameter (mm)	Area (mm^2)	Tensile modulus (GPa)	Ultimate strength (MPa)	Ultimate strain (%)	Shear strength (MPa)	Bond strength (MPa)
10	79	44.4 ± 0.3	1189 ± 74	2.7 ± 0.2	---	18.0 ± 0.2
12	113	45.3 ± 0.1	1162 ± 26	2.6 ± 0.1	245.2 ± 4.9	13.8 ± 1.9
16	201	48.7 ± 0.4	1173 ± 49	2.4 ± 0.1	225.9 ± 14.2	13.5 ± 1.6

Table 2 shows that the tested BFRP have a modulus of elasticity close to that of GFRP bars of Grade I (CSA S807, 2010). In addition, the BFRP bars exhibited maximum strain at failure ranging from 2.4 to 2.7% which is higher than the minimum value of 1.2% (CSA S807, 2010). Furthermore, the BFRP bars showed average transverse shear strength of 234.2±4.9 and 225.9±14.2 MPa for 12 and 16 mm-diameter, respectively. These values are higher than the 160 MPa limit provided by CSA S807 (2010). The bond strength was also satisfied because the three tested diameters (10, 12, and 16 mm) showed bond strengths higher than the 8 MPa specified by CSA S807 (2010). Thus, it could be concluded that the tested BFRP bars meet the mechanical properties requirements of CSA S807 (2010).

5 Bond-Depended Coefficient (k_b)

5.1 Crack width provisions

Calculation of crack width involves a common term that is included in the predicting equation—the bond-dependent coefficient (k_b)—to account for the degree of bond between FRP bars and the surrounding concrete. Different values for k_b were introduced by the available FRP design codes and guides for the different FRP reinforcing bars. Table 3 provides the available k_b values from design codes and guidelines. The following are the currently available equations in North American codes and guides for predicting the crack width in FRP-reinforced concrete members:

Table 3: Design recommendations for k_b values of different design codes and guides

ACI 440 (2006)	ISIS M-03 (2007)	CSA S6 (2010)
k_b values ranging from 0.60 to 1.72 (mean of 1.10) Conservative value of k_b = 1.4 (excluding smooth bars and grids)	In the absence of significant test data k_b = 1.2	Sand-coated FRP: k_b = 0.8 Deformed FRP: k_b = 1.0

5.1.1 ACI 440.1R-06 (ACI 440, 2006)

The maximum probable crack width for FRP-reinforced concrete members is calculated as follows:

[1] $$w = 2\,\frac{f_f}{E_f}\,\frac{h_2}{h_1}\,k_b\,\sqrt{d_c^{\,2} + (s/2)^2}$$

An analysis of crack width data by ACI Committee 440 on a variety of concrete cross-sections and FRP bars, fiber types, resin formulations, and surface treatments, yielded average k_b values ranging from 0.60 to 1.72, with a mean of 1.10.

5.1.2 CSA S6.1S1-10 (CSA S6, 2010)

The crack width has to be verified when the maximum tensile strain in FRP reinforcement under full service load exceeds 0.0015 using the following equation:

[2] $$w = 2\,\frac{f_f}{E_f}\,\frac{h_2}{h_1}\,k_b\,\sqrt{d_c^{\,2} + (s/2)^2}$$

The value of k_b should be determined experimentally, but, in the absence of test data, it may be taken as 0.8 for sand-coated and 1.0 for deformed FRP bars. In calculating d_c, the clear cover shall not be taken greater than 50 mm.

5.1.3 ISIS M-03 (2007)

ISIS design manual No. 3 predicts the crack width using Eq. [3]:

[3] $$w = 2.2\,\frac{f_f}{E_f}\,\frac{h_2}{h_1}\,k_b\,\sqrt{d_c^{\,2} A}$$

In the absence of significant test data, k_b =1.2 is recommended.

5.2 Beam specimens

The bond-depended coefficient (k_b) was determined through testing of three simply-supported beams reinforced with sand-coated BFRP of 10, 12, and 16 mm-diameter. The specimens and tests were designed in according with Annex S "*Test Method for Determining the Bond-Dependent Coefficient of Fibre-Reinforced Polymer (FRP) Rods*" of the CSA S806 (2012). The beams measured 3,100 mm long, 200 mm wide, and 300 mm deep. The beams were reinforced in tension with two BFRP bars (10, 12, and 16 mm-diameter) and in compression with two 10M steel bars. The beams were provided with closely spaced steel stirrups (10M @ 100 mm) in the shear spans to avoid shear failure. The constant moment zone was kept without stirrups to minimize the confinement contribution. Figure 5 shows the geometry and reinforcement details of the tested beams. The mechanical properties of the BFRP were provided in Table 2. However, Table 4 provides the details of the beam specimens.

Table 4: Details of beam specimens

Beam	f_c'	f_t	Reinforcement	ρ_f (%)	ρ_{fb} (%)	ρ_f/ρ_{fb}	E_fA_f (kN)
N2#3			2-10 mm bars	0.3	0.2	1.4	6952
N2#4	42.5±0.4	2.83±0.05	2-12 mm bars	0.4	0.2	1.8	10170
N2#5			2-16 mm bars	0.8	0.3	3.1	19698

The beams were constructed using a normal-weight, ready-mixed concrete with an average compressive strength of 42.5±0.4 MPa, determined from three 150×200 mm cylinders at the day of test. The tensile strength was also measured at the day of test through splitting test of three 150×200 mm cylinders and it was equal to 2.83±0.05 MPa.

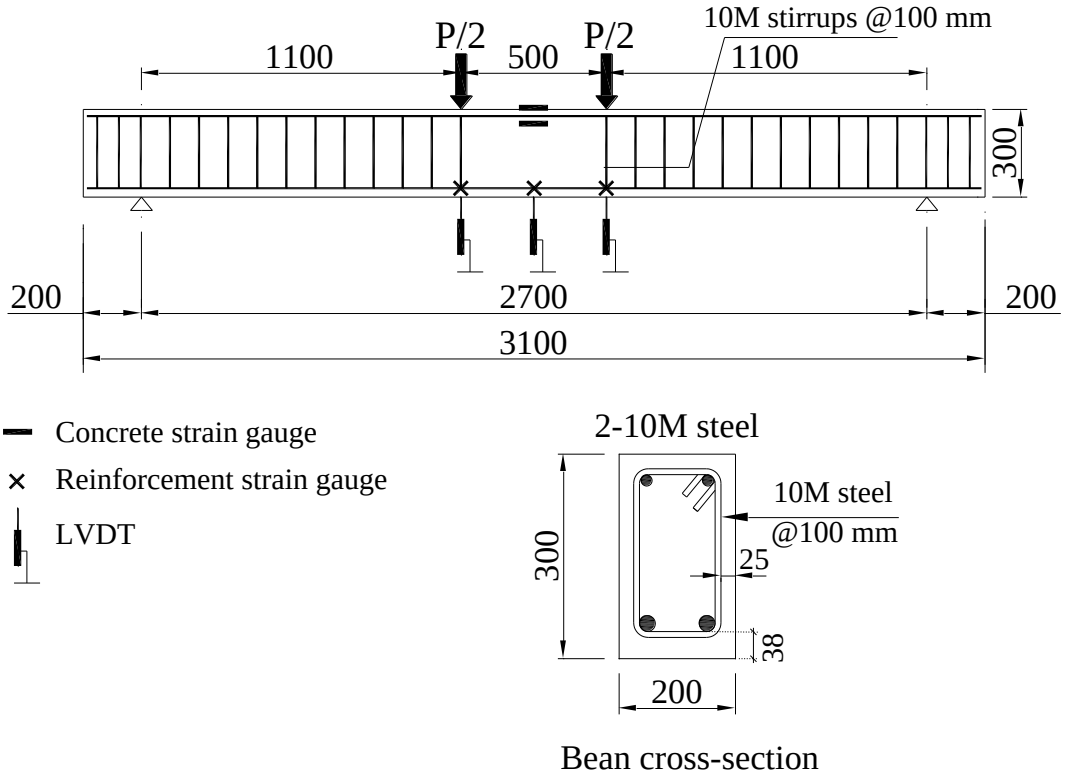

Figure 5: Details of beam specimens: geometry, reinforcement details, and instrumentation

5.3 Instrumentation and testing

Electrical-resistance strain gauges (10 mm and 60 mm long) were used to measure the tensile strains in the reinforcing bars and the concrete compressive strains at desired locations, respectively. Reinforcement strains gauges were glued to the BFRP bars at the beam midspan and at the two loading points. Concrete strain gauges, however, were glued to the top concrete surface at beam midspan. The midspan deflection was measured with two Linear Variable Displacement Transducers (LVDTs) with a 100 mm stroke, fastened to each side of the beam while the deflection of the beam at loading points were also measured using another two LVDTs. Figure 5 also shows the instrumentation of the beam specimens. In addition, the widths of the first three cracks were measured with a 50 mm stroke LVDTs. A data-acquisition module monitored by a computer was used to record the readings of the strain gauges, LVDTs and load cells at one reading per second rate. During loading, crack formation along the front face of the beams was marked and the corresponding loads were recorded.

The beams were tested in four-point bending over a simply-supported clear span of 2,700 mm and a shear span of 1,100 mm as shown in Figure 5. The load was monotonically applied using a 500 kN hydraulic actuator at a stroke-controlled rate of 0.6 mm/min. The test was paused when the first three flexural cracks appeared. Their initial crack widths were measured manually with a 50X hand-held optical microscope, and three LVDTs were installed to capture the crack width evolution with the load increase. Figure 6 shows the test setup during a beam test.

Figure 6: Test setup during a beam test

5.4 Test results and discussion

Figure 7 shows the three tested beams at failure. As the main objective of this paper is limited to the characterization and bond-dependent coefficient (k_b) determination, the presented results and discussions in this section will be limited only to the crack widths and k_b evaluation.

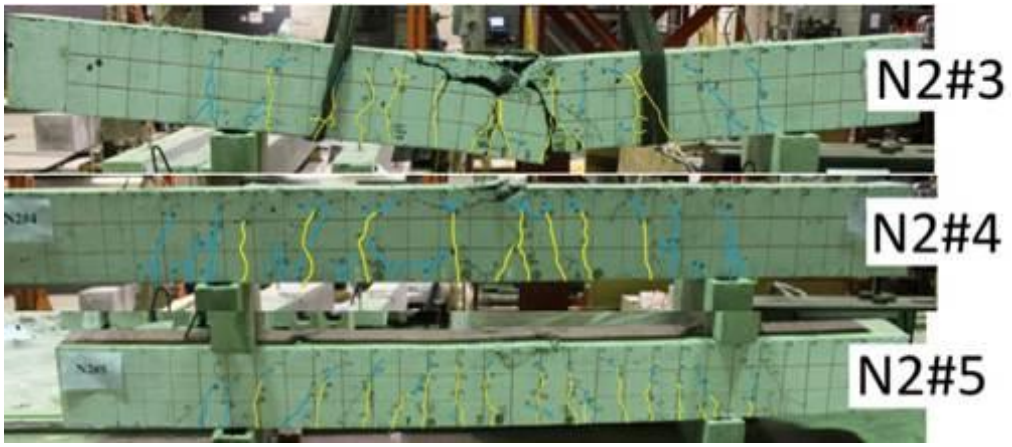

Figure 7: Tested beams at failure

Figure 8 shows the moment-crack width relationships of the three tested beams. The figure also introduces a comparison with the predicted crack widths using the available equations of ACI 440 (2006), ISIS M-03 (2007) and CSA S6 (2010). As mentioned earlier, three cracks in the constant moment zone were monitored and their widths were measured. The three cracks were used in the comparison for verifications. The k_b values that were used in the prediction were 1.4, 1.2, and 0.8 for ACI 440 (2006), ISIS M-03 (2007) and CSA S6 (2010), respectively (see Table 3). The comparisons in this figure indicate that ACI 440 (2006) and ISIS M-03 (2007) overestimate the crack widths in these beams. On the other hand, CSA S6 (2010) yielded good predictions for the three tested beams and the moment-crack width relationships were very close to the experimentally measured relationships.

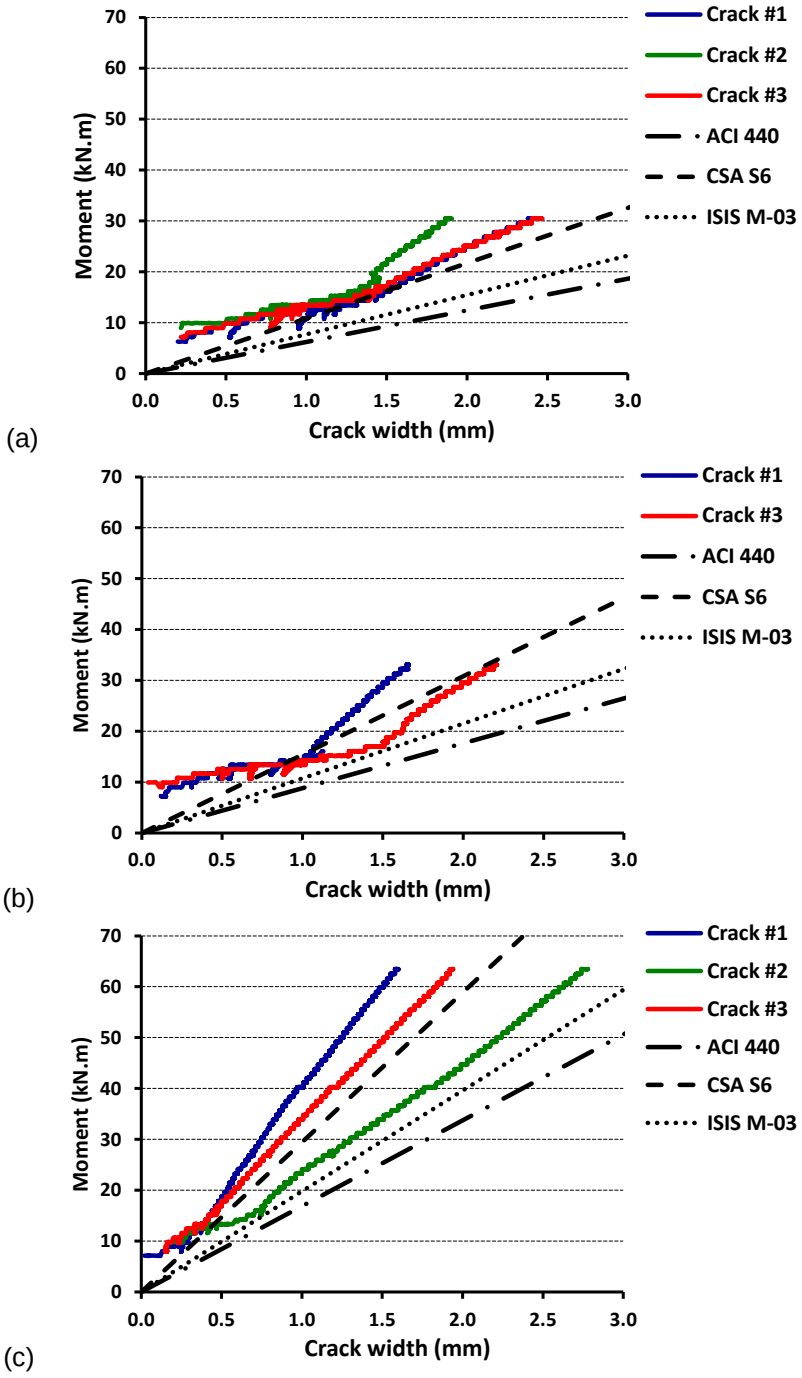

Figure 8: Experimental and predicted moment-crack width relationships: (a) Beam N2#3; (b) Beam N2#4; (c) Beam N2#5

The measured crack widths of the three tested beams were used in determining the bond-dependent coefficient (k_b) using Eqs. [1] to [3]. The calculations were made at 30% of the nominal capacity ($0.3M_n$) of the testes specimens as this value was reported as the service load level by many researchers (Mota et al. 2006; Bischoff 2009; El-Nemr et al. 2011). The k_b values were calculated according to the three cracks of each beam and the average value was introduced as shown in Table 5. The results indicate that the k_b value of the tested BFRP bars is close to the 0.8 recommended by the CSA S6 (2010). Thus, the predicated crack widths using CSA S6 (2010) were very close to the experimentally measured ones.

Table 5: Experimentally determined k_b values for BFRP bars at $0.3M_n$

	Calculated k_b value			
Beam	Crack #1	Crack #2	Crack #3	Average
N2#3	0.74	0.64	0.71	0.70
N2#4	0.79	N/A	0.97	0.88
N2#5	0.54	0.88	0.60	0.67
			Average	**0.74**

6 Concluding Remarks

This paper presented the result of an investigation conducted to characterize newly developed sand-coated basalt fiber-reinforced polymer (BFRP) bars and evaluate their bond-dependent coefficient (k_b). Based on the test results presented herein, the following conclusions are drawn:

- This preliminary study confirms that the developed basalt FRP (BFRP) bars meet the requirements of ACI 440 (2008) and CSA S807 (2010) concerning their physical and mechanical properties. The long-term performance of these bars in different environments and under different exposure conditions, however, has to be investigated.

- The measured bond-dependent coefficient (k_b) for the tested BFRP bars was 0.74. This value is very close to that of the CSA S6 (2010) for sand-coated FRP bars (k_b=0.8). Consequently, the predicted crack widths using CSA S6 (2010) provisions were very close to the experimentally measured ones.

7 Notation

The following symbols are used in this paper:

A = effective tension area of concrete surrounding the flexural tension reinforcement and bearing the same centroid as that reinforcement, divided by the number of bars (mm^2)
d_b = bar diameter (mm)
d_c = distance from extreme tension fiber to the center of the longitudinal bar or wire located closest thereto according to the code or guideline (mm)
E_f = modulus of elasticity of longitudinal FRP reinforcement (MPa)
E_s = modulus of elasticity of longitudinal steel reinforcement (MPa)
f'_c = compressive strength of the concrete (MPa)
f_f = stress in FRP reinforcement under specified loads (MPa)
f_t = tensile strength from cylinder-splitting test (MPa)
h_1 = distance from neutral axis to center of tensile reinforcement (mm)
h_2 = distance from neutral axis to extreme tension fiber (mm)
k_b = bond-dependent coefficient
s = spacing between the longitudinal reinforcement bars (mm)
T_g = glass transition temperature (^oC)
w = maximum crack width (mm)
ρ_f = longitudinal reinforcement ratio
ρ_{fb} = balanced longitudinal reinforcement ratio

8 Acknowledgments

The authors wish to acknowledge the financial support of the Natural Sciences and Engineering Research Council of Canada (NSERC), and the Fonds québécois de la recherche sur la nature et les technologies (FQRNT) of Quebec.

9 References

ACI Committee 440. 2004. Guide Test Methods for Fiber-Reinforced Polymers (FRPs) for Reinforcing or Strengthening Concrete Structures (ACI 440.3R-04). *American Concrete Institute*, Farmington Hills, USA, 40 p.

ACI Committee 440. 2008. Specification for Carbon and Glass Fiber-Reinforced Polymer Bar Materials for Concrete Reinforcement (ACI 440.6M-08). American Concrete Institute, Farmington Hills, MI, 6 p.

ASTM D3171. 2011. Standard Test Methods for Constituent Content of Composite*. American Society for Testing and Materials,* Conshohocken, USA, 10 p.

ASTM D3418. 2012. Standard Test Method for Transition Temperatures and Enthalpies of Fusion and Crystallization of Polymers by Differential Scanning Calorimetry. *American Society for Testing and Materials,* Conshohocken, USA, 7 p.

ASTM D5028. 1990. Standard Test Method for Curing Properties of Pultrusion Resin by Thermal Analysis. *American Society for Testing and Material*, Conshohocken, USA, 3 p.

ASTM D570. 2010. Standard Test Method for Water Absorption of Plastics*. American Society for Testing and Materials,* Conshohocken, USA. 4 p.

ASTM D7617. 2011. Standard Test Method for Transverse Shear Strength of Fiber-reinforced Polymer Matrix Composite Bars. *American Society for Testing and Materials,* Conshohocken, USA, 12 p.

ASTM E831. 2012. Standard Test Methods for Linear Thermal Expansion of Solids Materials by Thermomechanical Analysis. *American Society for Testing and Materials,* Conshohocken, USA, *4p.*

Bischoff, P.H., Gross, S., and Ospina, C.E. 2009. The Story behind Proposed Changes to the ACI 440 Deflection Requirements for FRP-Reinforced Concrete. ACI SP-264, *American Concrete Institute*, eds. Ospina, C., Bischoff, P., and Alkhrdaji, T., MI, pp. 53-76.

Canadian Standards Association (CSA). 2010. Canadian Highway Bridge Design Code. CAN/CSA S6-06, Rexdale, ON, Canada. 733 p.

Canadian Standards Association (CSA). 2010. Specification for Fibre-Reinforced Polymers (CAN/CSA S807–10). Rexdale, ON, Canada, 27 p.

Canadian Standards Association (CSA). 2012. Design and Construction of Building Structures with Fibre Reinforced Polymers (CAN/CSA S806-12). Rexdale, ON, Canada.

El-Nemr, A., Ahmed, E., and Benmokrane, B. 2011. Instantaneous Deflection of Slender Concrete Beams Reinforced with GFRP Bars. Proceedings of the 2nd International Engineering Mechanics and Materials Specialty Conference, CSCE, Ottawa, Ontario, June 14-17, (CD-ROM), 10 p.

ISIS Manual No. 3. 2007. Reinforced Concrete Structures with Fibre-Reinforced Polymers. ISIS Canada Research Network, University of Manitoba, Winnipeg, MB, 151 p.

Mota, C., Alminar, S., and Svecova, D. 2006. Critical Review of Deflection Formulas for FRP-RC Members. *Journal of Composites for Construction*, ASCE, 3(10): 183-194.